Published in final edited form as:
Biochemistry. 2012 October 2; 51(39): 7676–7684. doi:10.1021/bi3009888.

Phosphatidylethanolamine enhances amyloid fiber dependent membrane fragmentation

Michele F.M. Sciacca[†], **Jeffrey R. Brender**[†], **Dong-Kuk Lee**[†,‡], and **Ayyalusamy Ramamoorthy**[†,*]

[†]Departments of Biophysics and Chemistry, University of Michigan, Ann Arbor, Michigan 48109-1055 (USA)

[‡]Department of Fine Chemistry, Seoul National University of Science and Technology, Seoul, Korea 139-743

Abstract

The toxicity of amyloid-forming peptides has been hypothesized to reside in the ability of protein oligomers to interact with and disrupt the cell membrane. Much of the evidence for this hypothesis comes from *in vitro* experiments using model membranes. However, the accuracy of this approach depends on the ability of the model membrane to accurately mimic the cell membrane. The effect of membrane composition has been overlooked in many studies of amyloid toxicity in model systems. By combining measurements of membrane binding, membrane permeabilization, and fiber formation, we show that lipids with the phosphatidylethanolamine (PE) head group strongly modulate the membrane disruption induced by IAPP (islet amyloid polypeptide protein), an amyloidogenic protein involved in type II diabetes. Our results suggest that PE lipids hamper the interaction of prefibrillar IAPP with membranes, but enhance the membrane disruption correlated with the fiber growth on the membrane surface via a detergent-like mechanism. These findings provide insights into the mechanism of membrane disruption induced by IAPP, suggesting a possible role of PE also for other amyloids involved in other pathologies.

The accumulation of particular proteins into long fibrillar aggregates with a characteristic β-sheet structure known as amyloids is a common feature of many devastating aging-related pathologies.[1, 2] In type II diabetes mellitus, the main constituent of these aggregates is Islet Amyloid Polypeptide (IAPP),[3] a 37 residue peptide (sequence shown in Fig. 1) involved with insulin in glucose homeostasis.[4] Like many other amyloidogenic proteins, the aggregation of IAPP has been linked to cellular dysfunction and death.[5] Although the molecular mechanisms underlying the cytotoxicity of IAPP have not been fully elucidated, substantial evidence suggests that at least part of the toxicity of aggregates of IAPP and other amyloidogenic proteins is due to the disruption of the plasma and possibly organelle membranes during aggregation.[6–8] The exact mechanism of membrane disruption is not yet fully understood, although several studies have proposed either the formation of transmembrane oligomeric pores,[9–12] non-specific ion permeation caused by binding of

[*]Corresponding Author: Ayyalusamy Ramamoorthy, ramamoor@umich.edu, Phone: 734 647-6572.

ASSOCIATED CONTENT

Supporting Information Available

Procedures for LUV preparation, the dye leakage assays, and the ThT and lipid translocation assays. The CD spectra of IAPP in absence and presence of membrane, pyrene emission spectra from LUVs labeled symmetrically and asymmetrically with Py-PC, the effect of lipid concentration on the membrane disruption induced by IAPP and on the kinetics of IAPP fiber formation, and the concentration dependence of IAPP on membrane fragmentation are also included as supporting figures. This material is available free of charge via the Internet at http://pubs.acs.org.

oligomers to the membrane surface,[9] or a detergent-like membrane dissolution caused by the growth of amyloid fibrils on the membrane surface.[13–15]

Most mechanistic data on IAPP-induced membrane disruption at the molecular-level has come from *in vitro* studies on model membranes.[16] In most studies, a simplified membrane composition consisting of a single zwitterionic lipid (PC) and a single charged lipid (PG or PS) has been used.[13, 17–25] The net surface charge is an important property of the membrane that can strongly affect both the level of membrane disruption and the kinetics of amyloid formation. However, it is only one element in a large set of properties that define a realistic cell membrane mimetic. Alterations of other membrane properties have been shown to have large effects on the activity of other membrane active peptides and amyloid proteins.[26–29] Even subtle changes in membrane composition can give rise to synergistic effects and emergent phenomena. For example, α-synuclein, an amyloidogenic protein implicated in Parkinson's disease, binds weakly to PC and PE alone but strongly to PS/PE mixed membranes.[27] Similarly, phase separation in ternary lipid mixtures has been shown to strongly enhance membrane binding for a variety of amyloid proteins, including IAPP.[30, 31] Although the effects of some changes in membrane composition have been studied for IAPP, the effects of many have been unexplored.[32–34]

A particularly interesting membrane property in this context is the intrinsic curvature of the membrane, which is related to the shape of the individual lipids. The growth of amyloid fibers on the membrane can severely distort the shape of lipid vesicles, disrupting membrane integrity as the fiber elongates[14, 29, 35, 36] The stress on the membrane induced by this distortion is related to the composition of the membrane, as bending a membrane to a geometry opposed by its intrinsic curvature is an unfavorable process.[37] The ability several IAPP variants to disrupt β-cell membranes is correlated with the ability to cause negative (outward) curvature in the membrane, suggesting a possible role for intrinsic lipid curvature in membrane disruption by IAPP.[16, 38] Similarly, a recent paper shows that decreasing the content of lipids with phosphatidylethanolamine headgroup (PE), a lipid with an intrinsic negative curvature, in neuroblastoma cells reduces the toxicity of the amyloidogenic Aβ peptide implicated in Alzheimer disease.[39] While PE is localized primarily in the inner leaflet in cells,[40] where it would appear to be inaccessible to extracellular amyloid fibers, recent research suggests that the most damaging amyloid oligomers actually form intracellularly where they would have access to PE.[41, 42] These studies suggest that PE lipids, which are common constituents of cell membranes, could play an important role in membrane disruption by amyloidogenic peptides.

However, *in vivo* studies are complicated by the multiple roles lipids serve in the human body. Besides its structural role in the membrane, PE is also involved in several cellular processes that make a direct link between a toxicity decrease upon reduction of PE levels and membrane disruption difficult.[43] Here we explore this link by investigating the membrane disruption induced by IAPP on model membranes composed of lipids with different intrinsic curvature by adding either POPE or lysoPC, a single chain fatty acid with the opposite curvature of PE, into vesicles containing POPC and POPS. The percentage of POPS was kept constant at 30% to maintain an identical percentage of anionic lipids in each sample. Using a combination of dye leakage, ThT fluorescence, NMR, CD and spectrofluorimetric measurements, we observed that the presence of a PE lipid decreases membrane leakage induced by IAPP in its non-fibrillar form, but significantly increases leakage caused by IAPP fibers, correlating with the impact PE has on the affinity for each species for the membrane. Results from this study shed light on the mechanism at the root of the toxic effect of IAPP towards membranes and could be useful to investigate the behavior of other amyloid proteins.

Materials and methods

Materials

Human IAPP was purchased from AnaSpec (Fremont, CA) with a purity of 97 %. 1-palmitoyl-2-oleoyl-*sn*-glycero-3-phosphocholine (POPC), 1-palmitoyl-2-oleoyl-*sn*-glycero-3-phosphoethanolamine (POPE), 1-palmitoyl-2-oleoyl-*sn*-glycero-3-phospho-L-serine sodium salt (POPS), 1-palmitoyl-2-oleoyl-*sn*-glycero-3-phospho-(1'-*rac*-glycerol) sodium salt (POPG) and 1-palmitoyl-2-hydroxy-*sn*-glycero-3-phosphocholine (Lyso PC) were purchased from Avanti Polar lipids Inc. (Alabaster, AL). 1,1,1,3,3,3-hexafluoro-2-propanol (HFIP), L-α-Phosphatidylcholine, β-(pyren-1-YL)-decanoyl-γ-palmitoyl (Pyrene-PC), ferric chloride hexahydrate and ammonium thiocyanate were purchased from Sigma-Aldrich (St.Louis, MO). 6-Carboxyfluorescein was purchased from Fluka.

Preparation of lipid vesicles

POPC:POPS (7/3 molar ratio), POPE/POPC/POPS (3:4:3) and POPC/POPS/LysoPC (6.8/3/0.2) large unilamellar vesicles (LUVs) and 6-carboxyfluorescein dye filled LUVs were prepared using standard procedures as detailed in the Supporting Information.

Dye leakage assay

Membrane disruption was measured by the efflux of 6-carboxyfluorescein in a 96 well plate upon the addition of IAPP, as detailed in the Supporting Information.

ThT assay

The kinetics of amyloid formation were measured using the increase of fluorescence upon binding of the commonly used amyloid specific dye thioflavin T (ThT) as detailed in the Supporting Information.[44] Thioflavin T experiments were performed simultaneously with the dye leakage experiments, using the same microplate and the same IAPP stock solution.

CD experiments

Binding of prefibrillar IAPP to lipid vesicles was evaluated by CD by measuring the change in ellipicity of IAPP at 222 nm due to the conformational change from random coil to α-helix occurring upon membrane binding. DMSO could not be used to disaggregate the peptide for these experiments due to the absorbance of DMSO in the far UV. Instead, a 250 μM stock solution of IAPP was made in 100 μM HCl (pH 5) at 4 °C, a condition in which the peptide is disaggregated and stable.[45] The IAPP stock solution was then diluted to 25 μM in 10 mM phosphate buffer with 100 mM NaF (final pH 7.4), and then titrated with POPC/POPS and POPC/POPS/POPE LUVs.

The degree of binding to the membrane was measured by recording the ellipticity at 222 nm for 30 sec for each lipid to protein ratio. K_d was then calculated from the changes in the ellipicity by the one-site binding equation: $\Delta\varepsilon=\frac{[Lipid](\Delta\varepsilon_0-\Delta\varepsilon_\infty)}{K_d+[Lipid]}+\Delta\varepsilon_0$, where $\Delta\varepsilon_0$ is the ellipicity at 222 nm in the absence of lipid and $\Delta\varepsilon_\infty$ is the ellipicity at 222 nm at a saturating concentration of lipid. Spectra were collected at the initial and final points of the titration to be sure that the protein was in the random coil and α-helical conformations, respectively (Fig. S1 in supporting information).

NMR experiments

^{31}P NMR spectra were obtained from a Agilent 400 MHz solid-state NMR spectrometer using a spin-echo sequence (90°–τ–180°–τ, τ=60 μs) with 35 kHz proton decoupling, a 90° pulse duration of 5 μs and a recycle delay of 3 s. For the ^{31}P MAS spectra, control

multilamellar vesicles were prepared by hydrating 9 mg of lipid film in the appropriate molar ratio with 100 μl of 10 mM Tris buffer (pH 7.4 with 100 mM NaCl). Multilamellar vesicles containing the IAPP peptide were prepared similarly except the buffer also contained 1.178 mM IAPP (peptide to lipid molar ratio 1%). Samples packed in a 5 mm rotor were then spun with 4.5 kHz frequency at the magic angle; 200 transients with a recycle delay of 3s were averaged to obtain each ^{31}P NMR spectrum. For the oriented ^{31}P NMR spectra, a sample without the peptide was first prepared using 3 mg total of lipid as explained elsewhere.[46] After the acquisition of the initial spectrum, 200 μL of buffer (10 mM Tris, pH 7.4 with 100 mM NaCl) containing 196 μM IAPP (peptide to lipid molar ratio 1%) was added into the bag containing the lipid matrix and spectra were acquired at the times indicated. All spectra were processed using 10 Hz line broadening. All experiments were performed at 37 °C, and all spectra were referenced externally to phosphoric acid (0 ppm).

Lipid translocation assay

Lipid translocation was measured by the ratiometric change in fluorescence of pyrene labeled lipids that occurs after translocation due to dilution of the pyrene probe (Fig. S2),[47] as detailed in the Supporting information.

Membrane fragmentation assay

The amount of membrane fragmentation during fiber formation was quantified by measuring the lipid concentration in the supernatant after centrifugation of 1000 nm diameter LUVs incubated with IAPP for 5 hours in 10 mM phosphate buffer, 100 mM NaCl, pH 7.4. Lipid concentrations were measured colorimetrically by reaction with ammonium ferrothiocyanate following extraction in chloroform using a calibration curve prepared for each lipid composition. [48] Samples were spun at 14,000 rpm for 40 minutes to pellet non-fragmented vesicles. Each experiment was performed in triplicate.

Results

PE decreases membrane disruption during the lag-phase

Membrane disruption by IAPP is a two-stage process with distinct fiber dependent and fiber independent phases.[24] Amyloid fibril formation typically follows a sigmoidal time-course, with an initial lag-phase reflecting the time required to build up an appreciable population of energetically unfavorable nuclei before fiber formation can begin.[49] The second phase has the characteristic sigmoidal kinetics associated with fibril growth, and has been correlated with membrane damage through fiber growth on the membrane through seeding experiments and the use of amyloid inhibitors that block fiber growth.[14, 24, 29, 46] The origin of the first phase is less clear, but it is not dependent on fiber growth as some non-amyloidogenic analogues of IAPP show a similar effect.[17, 22, 23, 50] Instead, the first phase may reflect either the formation of channels or a non-specific bilayer thinning process [9, 17, 22, 23, 29, 50] observed for some membrane-lytic antimicrobial peptides.[51] Although the two-step mechanism has been reported for IAPP, evidence suggests many amyloid proteins may have similar fiber-dependent [52–55] and fiber-independent [56, 57] phases.

To investigate how incorporating lipids with different intrinsic curvature affects each stage of IAPP-induced membrane disruption, we followed membrane disruption by a dye-release assay (Fig. 2A) along with measurements of fibrillogenesis by the fiber-specific dye ThT (Fig. 3) at varying peptide to lipid ratios (Fig. S3 and S4). Fiber formation was slower in the presence of both membrane types than in solution, which is typical of fiber formation at the low peptide-to-lipid ratios used here.29, 58 A two-phase membrane disruption was found in all membrane types, although the kinetics and amount released in each phase differed

according to the membrane composition (Fig. 2A). In all samples, we observed an initial rapid increase in the fluorescence after the addition of IAPP that plateaues as time progressed (Figs. 2A and S3, dotted lines). This initial phase of membrane disruption can be accurately modeled by a double exponential (dotted lines), and reaches a level close to the final intensity before fiber formation begins for all samples (Figs. 2A, 3, S3, and S4). The degree of membrane disruption in both phases decreases as the peptide to lipid ratio is decreased, indicating membrane disruption is cooperative (Figs. 2A and S3).[17, 23]

Our results suggest that PE suppresses this initial phase of membrane disruption. The degree of membrane disruption in the samples without PE is nearly twice that of the PE samples at the 45 minute mark before the onset of fiber formation (8.3% vs. 3.6 % $p<.001$, Fig. 2A). In contrast to PE, the inclusion of 2% LysoPC into the vesicles had little effect on this phase of membrane disruption (Figs. 2A and S3), although LysoPC was incorporated at a much lower concentration. This finding is different from what has been observed for the antimicrobial peptide magainin 2, in which even low concentrations of LysoPC (1.5 %) strongly increase membrane disruption.[59]

PE enhances membrane disruption associated with fiber formation

After the completion of the first phase, the fluorescence rises again as a second process begins to disrupt the membrane (Fig. 2A).[24] The second phase of dye release shows the same sigmoidal kinetics as amyloid fibril formation (Fig. S5), indicating a correspondence between these two processes.[14] However, the two curves do not coincide, as might be expected if fiber formation is directly linked to the second phase (Fig. S6 and S7).[12, 14] In fact, the second phase occurs well after the ThT assay seems to indicate that fiber formation is essentially complete. However, the time difference between the two curves may stem from the differing sensitivities of each method. While the ThT assay measures fiber formation from all sources, the kinetics of the second phase of dye release are determined solely by the rate of fiber formation on the membrane. We therefore directly tested the influence of PE on membrane disruption by fibril growth by repeating the dye leakage experiment using preformed amyloid fibers to immediately seed amyloid growth.[14] Preformed amyloid fibers by themselves did not cause membrane disruption (Fig. S8), in agreement with previous reports.[14, 60] However, the addition of monomeric peptide to the preformed fibers caused an immediate increase in fluorescence, much larger for the sample with PE than that caused by monomeric IAPP alone (35.9% and 2.8% after 30 minutes respectively, Fig. 2A and B). The fraction of dye leaked from samples with PE is roughly three times the amount observed from those without PE (35.9% vs. 12.7%, $p<.001$). This result confirms PE strongly enhances membrane disruption by fiber growth on the membrane.

Prefibrillar IAPP binds less favorably to PE containing membranes

The dye-release assay results suggest that the presence of PE either alters the membrane binding affinity or alters the physical properties of the membrane to make it more or less susceptible to membrane disruption by different oligomeric states of the peptide. To investigate the first of these possibilities, we evaluated PE's effect on the membrane binding affinity by performing CD (circular dichroism) experiments and measuring the conformational change in IAPP from a random coil to α-helix that initially occurs upon binding to the membrane.[25] We followed this conformational transition by titrating a 25 μM solution of IAPP with a solution of vesicles and recording the ellipticity at 222 nm. Our results show that PE reduces the binding affinity of prefibrillar IAPP for the membrane (Fig. 4, K_d =190 μM ± 85 for PC/PS and K_d = 790 μM ± 270 for PE/PC/PS), consistent with the observation that the initial phase of dye release during the lag-phase is less in the presence of PE (Fig. 2). However, the amount of dye released in the fiber-dependent second phase is

significantly higher in the presence of PE, suggesting PE either binds the amyloid fiber more tightly than prefibrillar IAPP or membranes containing PE are particularly susceptible to fiber catalyzed membrane disruption.

IAPP amyloid fibers interact more strongly with PE than PC in mixed membranes

The CD analysis described above relies on the conformational change from the random coil to alpha-helical state that occurs when prefibrillar IAPP binds to the lipid bilayer. Since amyloid fibers remain in the β-sheet conformation when bound to the membrane, such an analysis cannot determine the interactions of the amyloid fiber with the membrane. Instead, ^{31}P solid-state NMR experiments were employed to directly measure the perturbation of each lipid component occurring when IAPP was added at high concentration to mixed bilayers (Fig. 5). POPC and POPS have very similar ^{31}P chemical shifts and cannot be resolved even by 2D NMR techniques.[61] For this reason, POPG was substituted for POPS in the ^{31}P NMR experiment, as they have the same charge and similar intrinsic curvature. Successive scans of aligned PC/PG/PE bilayers incubated with IAPP did not change significantly with incubation time (Fig. 5A), suggesting amyloid formation is rapid at the high peptide concentrations used and confirming the changes seen in Fig. 5 are reflective of the interaction of amyloid fibers with the bilayer.

In the absence of IAPP, the resonances are reasonably well resolved under magic angle spinning to identify the individual components of the bilayer (dotted lines, Fig. 5B and C). The addition of IAPP substantially broadens both the PC and PG resonances in the sample without PE (Fig. 5B) without a noticeable change in chemical shift, most likely reflecting shorter spin-spin relaxation times due to the motional restriction of the lipid headgroup upon peptide binding.[62] The broadening is roughly equal for PC and PG resonances, suggesting the membrane is either not phase separated or IAPP affects both lipids similarly.

The addition of PE to the membrane has a substantial effect on the broadening induced by IAPP binding. Like the membranes without PE, IAPP binding also causes broadening of the ^{31}P resonances of PE containing membranes (Fig. 5C). However, unlike the membranes without PE, the broadening is not equal for all lipids. IAPP binding causes significant broadening of the PG and PE resonances, suggesting a strong interaction with the headgroup of these lipids (Fig. 5C). By contrast, the resonance from PC was relatively unaffected (Fig. 5C). While it is difficult to quantitate the degree of binding only from the ^{31}P spectrum, the absence of significant broadening of the PC resonance indicates IAPP amyloid fibers have a less strong interaction with PC than either PG or PE in mixed membranes.

PE enhances detergent-like membrane fragmentation by IAPP

The dye release assay does not distinguish between membrane permeabilization through the formation of specific pores or by a detergent-like mechanism. Detergent-like membrane permeabilization is characterized by the fragmentation of the membrane into small micelle/vesicle like structures and can be evaluated by first sedimenting large unilamellar vesicles in the presence of IAPP and then measuring lipid concentrations in the supernatant by the Stewart assay.[48] We measured the lipid concentration of the supernatant before and 5 hours after the addition of IAPP (Fig. 6, concentration dependence shown in Fig. S9), as previous results suggested membrane fragmentation is related to amyloidogenesis.[46] In the absence of IAPP, only a small percentage of the total lipid concentration was in the supernatant, confirming that almost all of the lipids had sedimented after centrifugation. Five hours after the addition of IAPP, when fiber formation is expected to be complete, significantly more lipids were found in the supernatant of the PE samples, although the amount still represented a small fraction of the total lipid. In membranes without PE, the addition of IAPP only slightly elevated the soluble fraction of lipid (Fig. 6 and S9). This finding confirms that

vesicles containing PE are more prone to membrane fragmentation as the fibers form on the surface, consistent with higher dye release found in PE containing vesicles in the fiber-dependent membrane permeabilization phase and the high affinity of IAPP fiber to PE measured by NMR.

Fiber-dependent membrane disruption by IAPP occurs by a detergent-like mechanism involving a loss of membrane asymmetry

The low time-resolution of the centrifugation assay and the small amount of micelle-like lipids detected made its application to the initial phase of membrane disruption problematic. To test for solubilization of the membrane in this initial phase, we measured membrane fragmentation indirectly by tracking the loss of lipid bilayer asymmetry as a function of time, as it is expected that the formation of a micelle-like lipid aggregate or a toroidal pore will cause significant mixing of the two leaflets of a bilayer, while a traditional barrel-stave type pore will not.63 Accordingly, we tracked lipid translocation during the first phase of membrane disruption immediately after addition of peptide using a lipid labeled with a pyrene moiety (pyrene-PC) according to the method described by Müller et al.[47] The spectrum of pyrene is concentration dependent with the intensity ratio between the excimer and the monomer signal (I_E/I_M) decreasing with the pyrene concentration in an individual leaflet. When pyrene-PC is added asymmetrically to the outer leaflet of a vesicle, a loss of bilayer asymmetry will decrease the effective pyrene concentration in the bilayer and therefore reduce the I_E/I_M ratio.

Lipid translocation was not detected in either sample (PC/PS or PE/PC/PS) within the first 30 minutes after the addition of freshly dissolved peptide, in contrast to the positive control MSI-78, an antimicrobial peptide that is known to cause loss of lipid asymmetry at low concentrations through the formation of a toroidal-type pore (Fig. 7).[64] Since a significant amount of dye leakage occurs within this time-frame under similar conditions (see Fig. 2A), it is reasonable to conclude that the first phase of membrane disruption does not involve loss of lipid asymmetry.

The evaluation of lipid translocation in the fiber-dependent second phase was hampered by the level of flip-flop occurring in the absence of peptide during prolonged observation. To solve this problem, we repeated the lipid translocation assay by first incubating the LUVs sample with 1 μM preformed hIAPP fibers before the addition of monomeric IAPP. Fiber elongation occurs immediately in the presence of preformed fibers,[14] allowing observation without interference from the natural rate of flip-flop. For these samples, lipid translocation was detected immediately after the addition of monomeric IAPP (Fig. 7). Translocation is more evident for samples containing PE (Fig.7B), confirming the results obtained with the lipid sedimentation and dye release assays. This result suggests fiber dependent membrane disruption is enhanced by the presence of PE lipids and occurs through a detergent-like mechanism, while fiber-independent membrane disruption does not involve the fragmentation of the membrane.

Discussion

Although the exact mechanism by which IAPP disrupts membranes is disputed, current evidence suggests that it has both a fiber-independent first phase and fiber-dependent second phase. Depending on the concentration, either phase is sufficient to induce toxicity.[23, 50] Dye leakage experiments show that while PE initially suppresses the membrane disruption in the first phase, it results in greater membrane fragmentation during fiber formation (Fig. 2). The origins of this behavior correlate with the relative affinities of different oligomeric species of IAPP for PE. While prefibrillar IAPP has a weaker affinity for membranes containing PE, (Fig. 4) solid-state NMR shows that amyloid fibers of IAPP interact strongly

and specifically with PE in mixed bilayers (Fig. 5c). The strong interaction of amyloid fibers with PE during fiber formation is linked to greater amount of membrane disruption by a detergent-like mechanism and the appearance of small micelle-like protein-lipid aggregates (Fig. 6). This mechanism was not observed during the first phase of dye release, suggesting that the initial mechanism of disruption of membrane does not involve the formation of micelle-like structures or toroidal-type pores (Fig. 7).

From these experiments, it is apparent that the membrane composition modulates the relative affinity of different conformations of IAPP for the membrane, which in turn affects the degree of membrane permeabilization in each stage of membrane disruption. Why do the two conformations of IAPP show such a difference in binding to PE? In order for the membrane to remain in a stable flat lamellar phase, the relative cross-sectional area of the lipid headgroup and acyl chain regions of the bilayer must be similar.[37] PC is easily incorporated into flat lipid bilayers, as the cylindrical shape of the molecule ensures that the lipid molecules can be tightly packed against each other without a distortion of the bilayer shape. Phosphotidylethanolamine (PE), on the other hand, is wedge-shaped with a small headgroup compared to most other lipids (~40 $Å^2$ compared to ~80 $Å^2$ for PC).[65] The small headgroup of PE cannot be packed easily against other lipid headgroups in a lipid bilayer, which creates a stress in the membrane. This stress can be relieved by binding of peptides or proteins to the surface to the membrane, since a shallow insertion of the peptide into the bilayer can eliminate the void volume resulting from the smaller size of the PE headgroup.[65] A deeper insertion of the peptide is more unfavorable for PE than PC, as deep insertion creates additional curvature strain from the expansion of the hydrophobic core at the center of the membrane. From these considerations, we expect the inclusion of PE in the membrane should favor the binding of conformations of IAPP that bind near the membrane surface and disfavor those that insert into the hydrophobic core. LysoPC, which possesses the opposite curvature of PE, should favor the opposite localization, although it is difficult to incorporate large amounts of LysoPC into the membrane without affecting the membranes structural integrity.[59]

The relative binding affinities of the IAPP monomer and fiber follow this pattern. Freshly dissolved IAPP, which is largely monomeric, binds more tightly to pure PC membranes (see Fig. 4), as would be expected if the monomer of IAPP penetrated relatively deeply into the membrane. The position of the α-helical monomer of IAPP in the membrane is known with some certainty from EPR studies, which indicate the monomer binds parallel to the membrane surface.[58] The center of the helix (~6 Å in diameter) is positioned 6–9 Å below the phosphate group in POPS vesicles.[58] At this level, the top of the helix is in the interfacial region, 3–6 Å below the phosphate group, and the bottom of the helix extends significantly into the hydrophobic core.[58] This finding is supported by NMR studies which show that the peptide is significantly protected from the water-soluble paramagnetic Mn^{+2} ions, which suggests a deep insertion of the peptide.[66] Interestingly, the depth of insertion appears to be related to the ability to cause membrane disruption. When H18 is protonated or mutated to Arg, the peptide binds closer to the surface and loses most of its ability to disrupt membranes and cytotoxicity.[23] Similarly, the amyloidogenic $PAP_{248–286}$ peptide, which does not penetrate into membranes,[67] also does not cause membrane disruption or cytotoxicity.[68, 69]

While IAPP initially binds the membrane as an α-helix,[17, 25, 70] it is possible that the actual pores are formed from a minority of the peptide that is in the β-sheet or other conformation. In particular, pores formed from transmembrane β-hairpins have been proposed as a model for the channels formed by Aβ and other amyloidogenic proteins.[71] In this case, the influence of PE is likely to be indirect, as the lipid headgroup will likely have less influence on a transmembrane peptide. Since IAPP oligomers likely form on the membrane,[45, 72] PE

lipids can indirectly favor the formation of such transmembrane oligomers by increasing the amount of membrane bound IAPP.

In comparison to the IAPP monomer, few direct measurements of the positioning of amyloid fibers within the membrane have been made. However, deep insertion of amyloid fibers is virtually precluded by the substantial void volume created beneath the fiber upon insertion into the membrane. In the smaller monomeric peptide, the unfavorable increase in entropy caused by the creation of the void volume can be partially alleviated by the splaying of the lipid tails into the void volume. However, lipid splaying is less effective for amyloid fibers as the lipid tails cannot splay beneath the entire width of the fiber due to its large size. Consistent with this, indirect measurements consistently show that amyloid fibers localize at the surface and do not penetrate deeply into the membrane.[73, 74] Since these properties are generally true of all amyloid fibers, it is likely that the binding of most, if not all, amyloid fibers to the membrane is enhanced as the PE content of the membrane is increased. It is expected, therefore, that PE and other lipids with negative curvature (such as cardiolipid) will enhance fiber-dependent membrane damage for most, if not all, amyloidogenic proteins.

Supplementary Material

Refer to Web version on PubMed Central for supplementary material.

Acknowledgments

Funding source statements: This research was supported by funds from NIH (GM095640 to A. R.). D. K. Lee was supported by Basic Science Research Program through the National Research Foundation of Korea (NRF) funded by the Ministry of Education, Science and Technology (2009-0087836).

Abbreviations

PE	Phosphatidylethanolamine
IAPP	Islet Amyloid Polypeptide
PC	Phosphatidylcholine
PG	Phosphatidylglycerol
PS	Phosphatidylserine
NMR	Nuclear Magnetic Resonance
CD	Circular Dychroism
POPC	1-palmitoyl-2-oleoyl-*sn*-glycero-3-phosphocholine
POPE	1-palmitoyl-2-oleoyl-*sn*-glycero-3-phosphoethanolamine
POPS	1-palmitoyl-2-oleoyl-*sn*-glycero-3-phospho-L-serine sodium salt
POPG	1-palmitoyl-2-oleoyl-*sn*-glycero-3-phospho-(1'-*rac*-glycerol) sodium salt, LysoPC, 1-palmitoyl-2-hydroxy-*sn*-glycero-3-phosphocholine
HFIP	1,1,1,3,3,3-hexafluoro-2-propanol (HFIP), L-α-Phosphatidylcholine
Pyrene-PC	β-(pyren-1-YL)-decanoyl-γ-palmitoyl
ThT	Thioflavin T
LUV	Large Unilamellar Vesicles

References

1. Carrell RW, Lomas DA. Conformational disease. Lancet. 1997; 350:134–138. [PubMed: 9228977]
2. Chiti F, Dobson CM. Protein misfolding, functional amyloid, and human disease. Annu. Rev. Biochem. 2006; 75:333–366. [PubMed: 16756495]
3. Westermark P, Wernstedt C, Wilander E, Hayden DW, Obrien TD, Johnson KH. Amyloid fibrils in human insulinoma and islets of langerhans of the diabetic cat are derived from a neuropeptide-like protein also present in normal islet cells. Proc. Natl. Acad. Sci. U. S. A. 1987; 84:3881–3885. [PubMed: 3035556]
4. Woods SC, Lutz TA, Geary N, Langhans W. Pancreatic signals controlling food intake; insulin, glucagon and amylin. Philos. Trans. R. Soc. Lond. B Biol. Sci. 2006; 361:1219–1235. [PubMed: 16815800]
5. Westermark P, Andersson A, Westermark GT. Islet amyloid polypeptide, islet amyloid, and diabetes mellitus. Physiol. Rev. 2011; 91:795–826. [PubMed: 21742788]
6. Kayed R, Sokolov Y, Edmonds B, McIntire TM, Milton SC, Hall JE, Glabe CG. Permeabilization of lipid bilayers is a common conformation-dependent activity of soluble amyloid oligomers in protein misfolding diseases. J. Biol. Chem. 2004; 279:46363–46366. [PubMed: 15385542]
7. Haataja L, Gurlo T, Huang CJ, Butler PC. Islet amyloid in type 2 diabetes, and the toxic oligomer hypothesis. Endocr. Rev. 2008; 29:302–316.
8. Hebda JA, Miranker AD. The interplay of catalysis and toxicity by amyloid intermediates on lipid bilayers: Insights from type II diabetes. Annu. Rev. Biophys. Biomol. Struct. 2009; 38:125–152.
9. Last NB, Rhoades E, Miranker AD. Islet amyloid polypeptide demonstrates a persistent capacity to disrupt membrane integrity. Proc. Natl. Acad. Sci. U. S. A. 2011; 108:9460–9465. [PubMed: 21606325]
10. Lashuel HA, Lansbury PT. Are amyloid diseases caused by protein aggregates that mimic bacterial pore-forming toxins? Q. Rev. Biophys. 2006; 39:167–201. [PubMed: 16978447]
11. Anguiano M, Nowak RJ, Lansbury PT. Protofibrillar islet amyloid polypeptide permeabilizes synthetic vesicles by a pore-like mechanism that may be relevant to type II diabetes. Biochemistry. 2002; 41:11338–11343. [PubMed: 12234175]
12. La Rosa C, Scalisi S, Sciacca MFM, Zhavnerko G, Grasso DM, Marletta G. Self-assembling pathway of hIAPP fibrils within lipid bilayers. Chembiochem. 2010; 11:1856–1859. [PubMed: 20672280]
13. Sparr E, Engel MFM, Sakharov DV, Sprong M, Jacobs J, de Kruijff B, Hoppener JWM, Killian JA. Islet amyloid polypeptide-induced membrane leakage involves uptake of lipids by forming amyloid fibers. FEBS Lett. 2004; 577:117–120. [PubMed: 15527771]
14. Engel MF, Khemtemourian L, Kleijer CC, Meeldijk HJ, Jacobs J, Verkleij AJ, de Kruijff B, Killian JA, Hoppener JW. Membrane damage by human islet amyloid polypeptide through fibril growth at the membrane. Proc. Natl. Acad. Sci. U. S. A. 2008; 105:6033–6038. [PubMed: 18408164]
15. Green JD, Kreplak L, Goldsbury C, Blatter XL, Stolz M, Cooper GS, Seelig A, Kist-Ler J, Aebi U. Atomic force microscopy reveals defects within mica supported lipid bilayers induced by the amyloidogenic human amylin peptide. J. Mol. Biol. 2004; 342:877–887. [PubMed: 15342243]
16. Brender JR, Salamekh S, Ramamoorthy A. Membrane disruption and early events in the aggregation of the diabetes related peptide IAPP from a molecular perspective. Acc. Chem. Res. 2012; 45:454–462. [PubMed: 21942864]
17. Knight JD, Hebda JA, Miranker AD. Conserved and cooperative assembly of membrane-bound alpha-helical states of islet amyloid polypeptide. Biochemistry. 2006; 45:9496–9508. [PubMed: 16878984]
18. Knight JD, Miranker AD. Phospholipid catalysis of diabetic amyloid assembly. J. Mol. Biol. 2004; 341:1175–1187. [PubMed: 15321714]
19. Evers F, Jeworrek C, Tiemeyer S, Weise K, Sellin D, Paulus M, Struth B, Tolan M, Winter R. Elucidating the mechanism of lipid membrane-induced IAPP fibrillogenesis and its inhibition by the red wine compound resveratrol: A synchrotron x-ray reflectivity study. J. Am. Chem. Soc. 2009; 131:9516–9521. [PubMed: 19583433]

20. Sellin D, Yan LM, Kapurniotu A, Winter R. Suppression of IAPP fibrillation at anionic lipid membranes via IAPP-derived amyloid inhibitors and insulin. Biophys. Chem. 2010; 150:73–79. [PubMed: 20153100]
21. Engel MFM, Yigittop H, Elgersma RC, Rijkers DTS, Liskamp RMJ, de Kruijff B, Hoppener JWM, Killian JA. Islet amyloid polypelptide inserts into phospholipid monolayers as monomer. J. Mol. Biol. 2006; 356:783–789. [PubMed: 16403520]
22. Brender JR, Lee EL, Cavitt MA, Gafni A, Steel DG, Ramamoorthy A. Amyloid fiber formation and membrane disruption are separate processes localized in two distinct regions of IAPP, the type-2-diabetes-related peptide. J. Am. Chem. Soc. 2008; 130:6424–6429. [PubMed: 18444645]
23. Brender JR, Hartman K, Reid KR, Kennedy RT, Ramamoorthy A. A single mutation in the nonamyloidogenic region of islet amyloid polypeptide greatly reduces toxicity. Biochemistry. 2008; 47:12680–12688. [PubMed: 18989933]
24. Brender JR, Lee EL, Hartman K, Wong PT, Ramamoorthy A, Steel DG, Gafni A. Biphasic effects of insulin on islet amyloid polypeptide membrane disruption. Biophys. J. 2011; 100:685–692. [PubMed: 21281583]
25. Jayasinghe SA, Langen R. Lipid membranes modulate the structure of islet amyloid polypeptide. Biochemistry. 2005; 44:12113–12119. [PubMed: 16142909]
26. Grudzielanek S, Smirnovas V, Winter R. The effects of various membrane physical-chemical properties on the aggregation kinetics of insulin. Chem. Phys. Lipids. 2007; 149:28–39. [PubMed: 17603032]
27. Jo EJ, McLaurin J, Yip CM, St George-Hyslop P, Fraser PE. Alpha-synuclein membrane interactions and lipid specificity. J. Biol. Chem. 2000; 275:34328–34334. [PubMed: 10915790]
28. Zhu M, Li J, Fink AL. The association of alpha-synuclein with membranes affects bilayer structure, stability, and fibril formation. J. Biol. Chem. 2003; 278:40186–40197. [PubMed: 12885775]
29. Sciacca MF, Kotler SA, Brender JR, Chen J, Lee DK, Ramamoorthy A. Two-step mechanism of membrane disruption by abeta through membrane fragmentation and pore formation. Biophys J. 103:702–710. [PubMed: 22947931]
30. Radovan D, Opitz N, Winter R. Fluorescence microscopy studies on islet amyloid polypeptide fibrillation at heterogeneous and cellular membrane interfaces and its inhibition by resveratrol. FEBS Lett. 2009; 583:1439–1445. [PubMed: 19344717]
31. Weise K, Radovan D, Gohlke A, Opitz N, Winter R. Interaction of hIAPP with model raft membranes and pancreatic beta-cells: Cytotoxicity of hIAPP oligomers. Chembiochem. 2010; 11:1280–1290. [PubMed: 20440729]
32. Wakabayashi M, Matsuzaki K. Ganglioside-induced amyloid formation by human islet amyloid polypeptide in lipid rafts. FEBS Lett. 2009; 583:2854–2858. [PubMed: 19647738]
33. Cho WJ, Trikha S, Jeremic AM. Cholesterol regulates assembly of human islet amyloid polypeptide on model membranes. J. Mol. Biol. 2009; 393:765–775. [PubMed: 19720065]
34. Trikha S, Jeremic AM. Clustering and internalization of toxic amylin oligomers in pancreatic cells require plasma membrane cholesterol. J. Biol. Chem. 2011; 286:36086–36097. [PubMed: 21865171]
35. Morita M, Vestergaard M, Hamada T, Takagi M. Real-time observation of model membrane dynamics induced by Alzheimer's amyloid beta. Biophys. Chem. 2010; 147:81–86. [PubMed: 20060637]
36. Domanov YA, Kinnunen PKJ. Islet amyloid polypeptide forms rigid lipid-protein amyloid fibrils on supported phospholipid bilayers. J. Mol. Biol. 2008; 376:42–54. [PubMed: 18155730]
37. Lundbaek JA, Collingwood SA, Ingolfsson HI, Kapoor R, Andersen OS. Lipid bilayer regulation of membrane protein function: Gramicidin channels as molecular force probes. J. R. Soc. Interface. 2010; 7:373–395. [PubMed: 19940001]
38. Smith PES, Brender JR, Ramamoorthy A. Induction of negative curvature as a mechanism of cell toxicity by amyloidogenic peptides: The case of islet amyloid polypeptide. J. Am. Chem. Soc. 2009; 131:4470–4478. [PubMed: 19278224]

39. Cazzaniga E, Bulbarelli A, Lonati E, Orlando A, Re F, Gregori M, Masserini M. Aβ peptide toxicity is reduced after treatments decreasing phosphatidylethanolamine content in differentiated neuroblastoma cells. Neurochem. Res. 2011; 36:863–869. [PubMed: 21287268]
40. Janmey PA, Kinnunen PKJ. Biophysical properties of lipids and dynamic membranes. Trends Cell Biol. 2006; 16:538–546. [PubMed: 16962778]
41. Walsh DM, Klyubin I, Fadeeva JV, Cullen WK, Anwyl R, Wolfe MS, Rowan MJ, Selkoe DJ. Naturally secreted oligomers of amyloid β protein potently inhibit hippocampal long-term potentiation in vivo. Nature. 2002; 416:535–539. [PubMed: 11932745]
42. Lin CY, Gurlo T, Kayed R, Butler AE, Haataja L, Glabe CG, Butler PC. Toxic human islet amyloid polypeptide (h-IAPP) oligomers are intracellular, and vaccination to induce anti-toxic oligomer antibodies does not prevent h-IAPP-induced beta-cell apoptosis in h-IAPP transgenic mice. Diabetes. 2007; 56:1324–1332. [PubMed: 17353506]
43. Vance JE. Thematic review series: Glycerolipids. Phosphatidylserine and phosphatidylethanolamine in mammalian cells: Two metabolically related aminophospholipids. J. Lipid Res. 2008; 49:1377–1387. [PubMed: 18204094]
44. Brender JR, Hartman K, Nanga RP, Popovych N, de la Salud Bea R, Vivekanandan S, Marsh EN, Ramamoorthy A. Role of zinc in human islet amyloid polypeptide aggregation. J. Am. Chem. Soc. 2010; 132:8973–8983. [PubMed: 20536124]
45. Soong R, Brender JR, Macdonald PM, Ramamoorthy A. Association of highly compact type II diabetes related islet amyloid polypeptide intermediate species at physiological temperature revealed by diffusion NMR spectroscopy. J. Am. Chem. Soc. 2009; 131:7079–7085. [PubMed: 19405534]
46. Brender JR, Durr UHN, Heyl D, Budarapu MB, Ramamoorthy A. Membrane fragmentation by an amyloidogenic fragment of human islet amyloid polypeptide detected by solid-state NMR spectroscopy of membrane nanotubes. Biochim. Biophys. Acta. 2007; 1768:2026–2029. [PubMed: 17662957]
47. Muller P, Schiller S, Wieprecht T, Dathe M, Herrmann A. Continuous measurement of rapid transbilayer movement of a pyrene-labeled phospholipid analogue. Chem. Phys. Lipids. 2000; 106:89–99. [PubMed: 10878238]
48. Stewart JC. Colorimetric determination of phospholipids with ammonium ferrothiocyanate. Anal. Biochem. 1980; 104:10–14. [PubMed: 6892980]
49. Kodaka M. Requirements for generating sigmoidal time-course aggregation in nucleation-dependent polymerization model. Biophys. Chem. 2004; 107:243–253. [PubMed: 14967239]
50. Magzoub M, Miranker AD. Concentration-dependent transitions govern the subcellular localization of islet amyloid polypeptide. FASEB J. 26:1228–1238. [PubMed: 22183778]
51. Bechinger B, Lohner K. Detergent-like actions of linear amphipathic cationic antimicrobial peptides. Biochim. Biophys. Acta. 2006; 1758:1529–1539. [PubMed: 16928357]
52. Reynolds NP, Soragni A, Rabe M, Verdes D, Liverani E, Handschin S, Riek R, Seeger S. Mechanism of membrane interaction and disruption by alpha-synuclein. J. Am. Chem. Soc. 2011; 133:19366–19375. [PubMed: 21978222]
53. Jan A, Adolfsson O, Allaman I, Buccarello AL, Magistretti PJ, Pfeifer A, Muhs A, Lashuel HA. A beta 42 neurotoxicity is mediated by ongoing nucleated polymerization process rather than by discrete a beta 42 species. J. Biol. Chem. 2011; 286:8585–8596. [PubMed: 21156804]
54. Pellarin R, Friedman R, Caflisch A. Amyloid aggregation on lipid bilayers and its impact on membrane permeability. J. Mol. Biol. 2009; 387:407–415. [PubMed: 19133272]
55. Michikawa M, Gong JS, Fan QW, Sawamura N, Yanagisawa K. A novel action of Alzheimer's amyloid beta-protein (Aβ): Oligomeric Aβ promotes lipid release. J. Neurosci. 2001; 21:7226–7235. [PubMed: 11549733]
56. Kagan BL, Thundimadathil J. Amyloid peptide pores and the beta sheet conformation. Proteins. 2010; 677:150–167.
57. Jang HB, Zheng J, Lal R, Nussinov R. New structures help the modeling of toxic amyloid beta ion channels. Trends Biochem. Sci. 2008; 33:91–100. [PubMed: 18182298]

58. Apostolidou M, Jayasinghe SA, Langen R. Structure of alpha-helical membrane-bound hIAPP and its implications for membrane-mediated misfolding. J. Biol. Chem. 2008; 283:17205–17210. [PubMed: 18442979]
59. Matsuzaki K, Sugishita K, Ishibe N, Ueha M, Nakata S, Miyajima K, Epand RM. Relationship of membrane curvature to the formation of pores by magainin 2. Biochemistry. 1998; 37:11856–11863. [PubMed: 9718308]
60. Konarkowska B, Aitken JF, Kistler J, Zhang SP, Cooper GJS. The aggregation potential of human amylin determines its cytotoxicity towards islet beta-cells. FEBS J. 2006; 273:3614–3624. [PubMed: 16884500]
61. Warschawski DE, Fellmann P, Devaux PF. High resolution p-31-h-1 two-dimensional nuclear magnetic resonance spectra of unsonicated lipid mixtures spinning at the magic-angle. Euro. Biophys. J. Biophys. Lett. 1996; 25:131–137.
62. Lindstrom F, Bokvist M, Sparrman T, Grobner G. Association of amyloid-beta peptide with membrane surfaces monitored by solid state NMR. Phys. Chem. Chem. Phys. 2002; 4:5524–5530.
63. Butterfield SM, Lashuel HA. Amyloidogenic protein membrane interactions: Mechanistic insight from model systems. Angew. Chem. Int. Ed. 2010; 49:5628–5654.
64. Hallock KJ, Lee DK, Ramamoorthy A. Msi-78, an analogue of the magainin antimicrobial peptides, disrupts lipid bilayer structure via positive curvature strain. Biophys. J. 2003; 84:3052–3060. [PubMed: 12719236]
65. Heller WT, He K, Ludtke SJ, Harroun TA, Huang HW. Effect of changing the size of lipid headgroup on peptide insertion into membranes. Biophys. J. 1997; 73:239–244. [PubMed: 9199788]
66. Nanga RPR, Brender JR, Xu JD, Veglia G, Ramamoorthy A. Structures of rat and human islet amyloid polypeptide IAPP(1–19) in micelles by NMR spectroscopy. Biochemistry. 2008; 47:12689–12697. [PubMed: 18989932]
67. Nanga RPR, Brender JR, Vivekanandan S, Popovych N, Ramamoorthy A. NMR structure in a membrane environment reveals putative amyloidogenic regions of the SEVI precursor peptide PAP(248–286). J. Am. Chem. Soc. 2009; 131:17972–17979. [PubMed: 19995078]
68. Brender JR, Hartman K, Gottler LM, Cavitt ME, Youngstrom DW, Ramamoorthy A. Helical conformation of the SEVI precursor peptide PAP(248–286), a dramatic enhancer of HIV infectivity, promotes lipid aggregation and fusion. Biophys. J. 2009; 97:2474–2483. [PubMed: 19883590]
69. Munch J, Rucker E, Standker L, Adermann K, Goffinet C, Schindler M, Wildum S, Chinnadurai R, Rajan D, Specht A, Gimenez-Gallego G, Sanchez PC, Fowler DM, Koulov A, Kelly JW, Mothes W, Grivel JC, Margolis L, Keppler OT, Forssmann WG, Kirchhoff F. Semen-derived amyloid fibrils drastically enhance HIV infection. Cell. 2007; 131:1059–1071. [PubMed: 18083097]
70. Nanga RPR, Brender JR, Vivekanandan S, Ramamoorthy A. Structure and membrane orientation of IAPP in its natively amidated form at physiological pH in a membrane environment. Biochim. Biophys. Acta. 2011; 1808:2337–2342. [PubMed: 21723249]
71. Jang H, Arce FT, Ramachandran S, Capone R, Lal R, Nussinov R. Beta-barrel topology of Alzheimer's beta-amyloid ion channels. J. Mol. Biol. 2010; 404:917–934. [PubMed: 20970427]
72. Vaiana SM, Ghirlando R, Yau WM, Eaton WA, Hofrichter J. Sedimentation studies on human amylin fail to detect low-molecular-weight oligomers. Biophys. J. 2008; 94:L45–L47. [PubMed: 18223003]
73. Zhang YJ, Shi JM, Bai CJ, Wang H, Li HY, Wu Y, Ji SR. Intra-membrane oligomerization and extra-membrane oligomerization of amyloid-beta peptide are competing processes as a result of distinct patterns of motif interplay. J. Biol. Chem. 2012; 287:748–756. [PubMed: 22105077]
74. Lee CC, Sun Y, Huang HW. How type II diabetes-related islet amyloid polypeptide damages lipid bilayers. Biophys. J. 2012; 102:1059–1068. [PubMed: 22404928]

Figure 1.
Amino acid sequence of IAPP. IAPP is amidated in its physiologically occuring form and contains a disulfide bond between Cys2-Cys7.

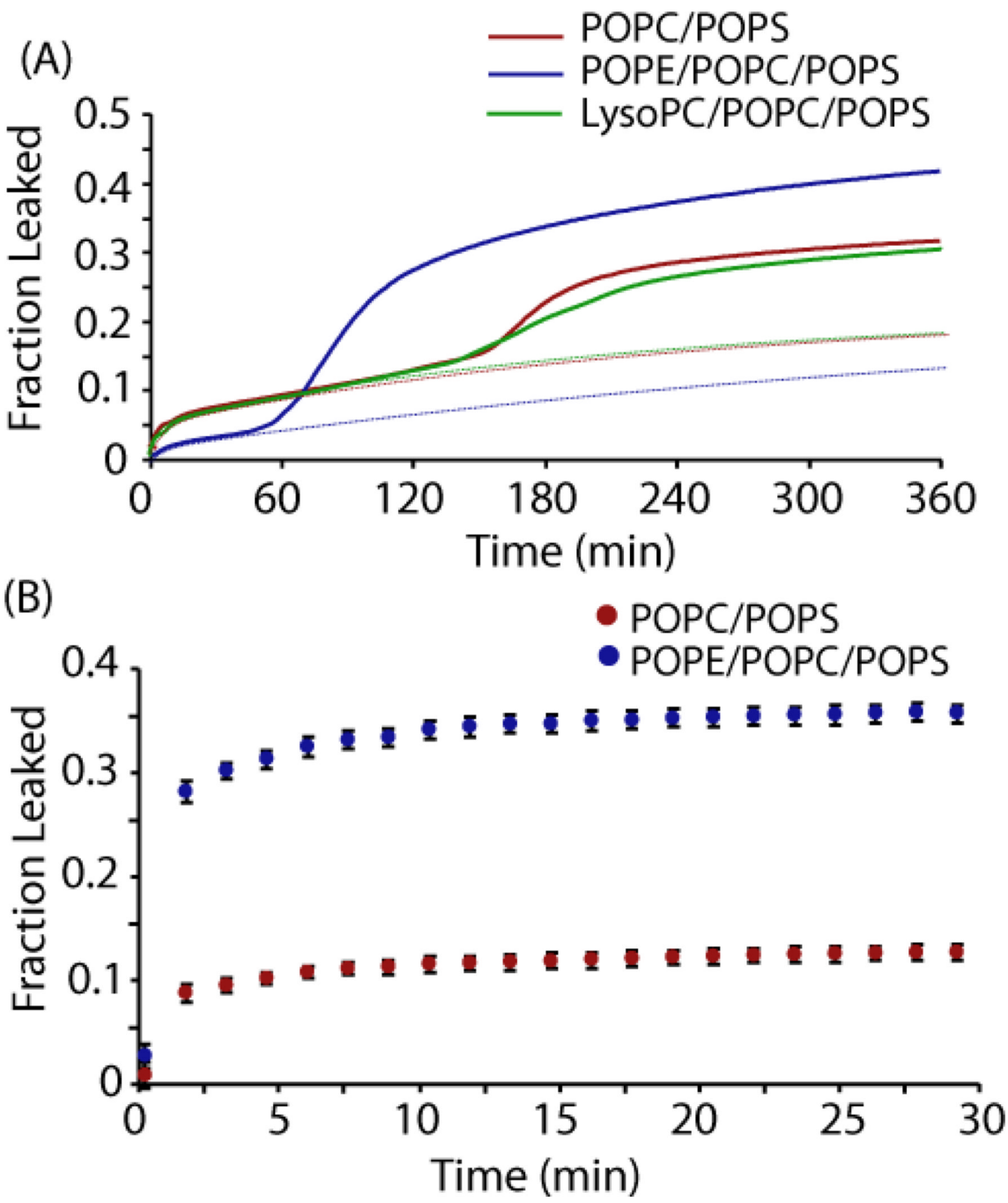

Figure 2.

Membrane disruption induced by IAPP. **(A)** Release of 6-carboxyfluorescein from large unilamellar vesicles (LUVs) composed of 250 μM POPC/POPS (7/3 molar ratio), POPE/POPC/POPS (3/4/3), or POPC/POPS/LysoPC (6.8/3/0.2) induced by 2.5 μM IAPP. The initial phase of membrane disruption was fitted with a double exponential curve (dotted lines). The presence of POPE decreases the amount of dye released during the first phase and markedly increases the efficiency of dye release during the second phase. **(B)** Release of 6-carboxyfluorescein from seeded fibril growth. Error bars indicate the standard error of

measurement. All experiments were performed in triplicate at 25 °C in 10 mM phosphate buffer, 100 mM NaCl, pH 7.4.

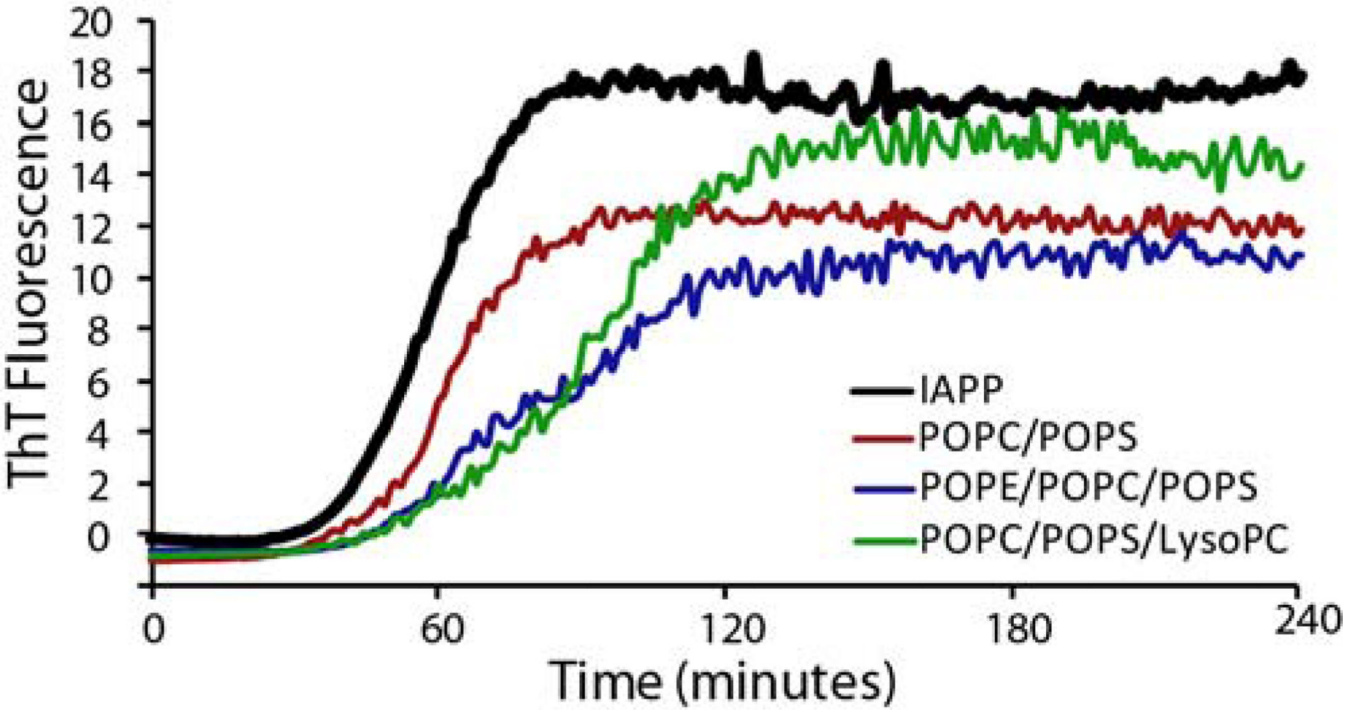

Figure 3.

IAPP fiber formation kinetics measured by ThT fluorescence. Fiber formation was measured in the presence of 250 μM of POPC/POPS (7:3 molar ratio), POPE/POPC/POPS (3/4/3), POPC/POPS/LysoPC (6.8/3/0.2) vesicles. Fiber formation in the absence of lipids is indicated by the black line. IAPP concentration was 2.5 μM for all samples. Experiments were performed at 25 °C in 10 mM phosphate buffer, 100 mM NaCl, pH 7.4. Results are the average of three experiments.

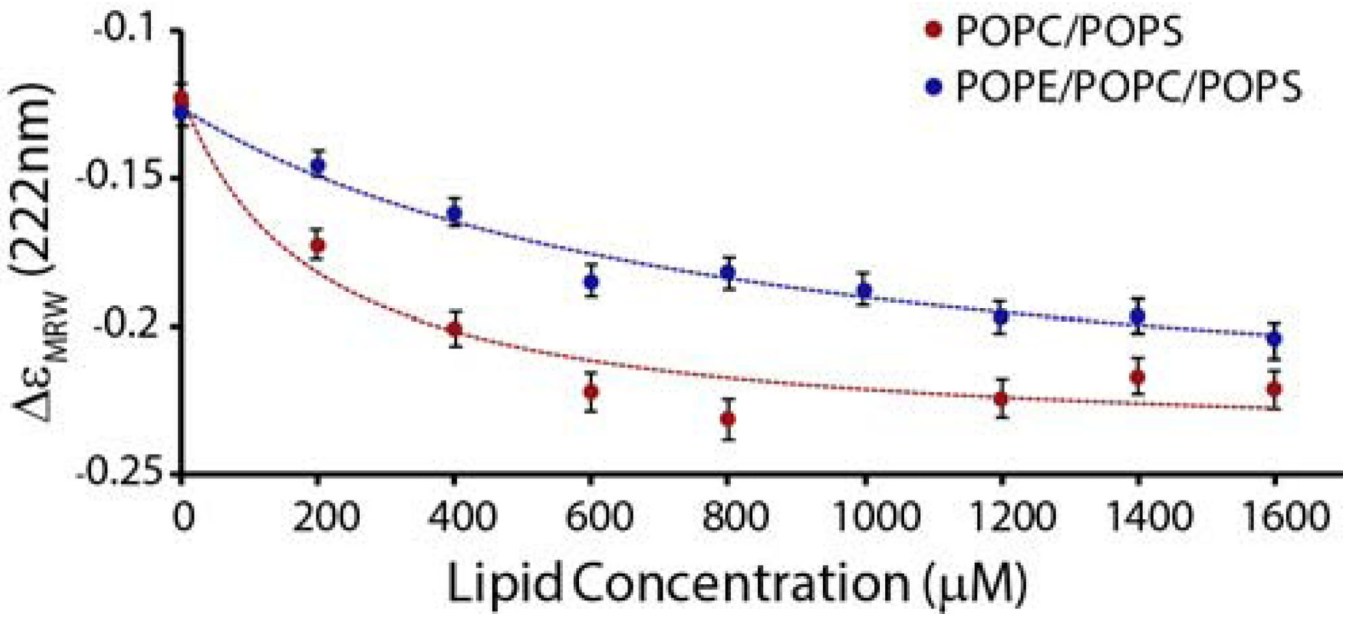

Figure 4.

Binding of prefibrillar IAPP to lipid vesicles. Changes in molar ellipicity at 222 nm arising from the coil-to-helix conformational change upon membrane binding as a function of the lipid concentration. 25 μM of freshly dissolved IAPP was titrated with the indicated concentrations of 7/3 POPC/POPS (filled circles) and 3/4/3 POPE/POPC/POPS (open circles) LUVs. The final conformation of IAPP is similar in both membranes (Fig. S1). Lines represent a binding isotherm to each dataset. Experiments were performed at 25 °C in 10 mM phosphate buffer, 100 mM NaF pH 7.4. Measurements represent the average of 30 measurements over 30 seconds, error bars indicate the standard deviation of this measurement.

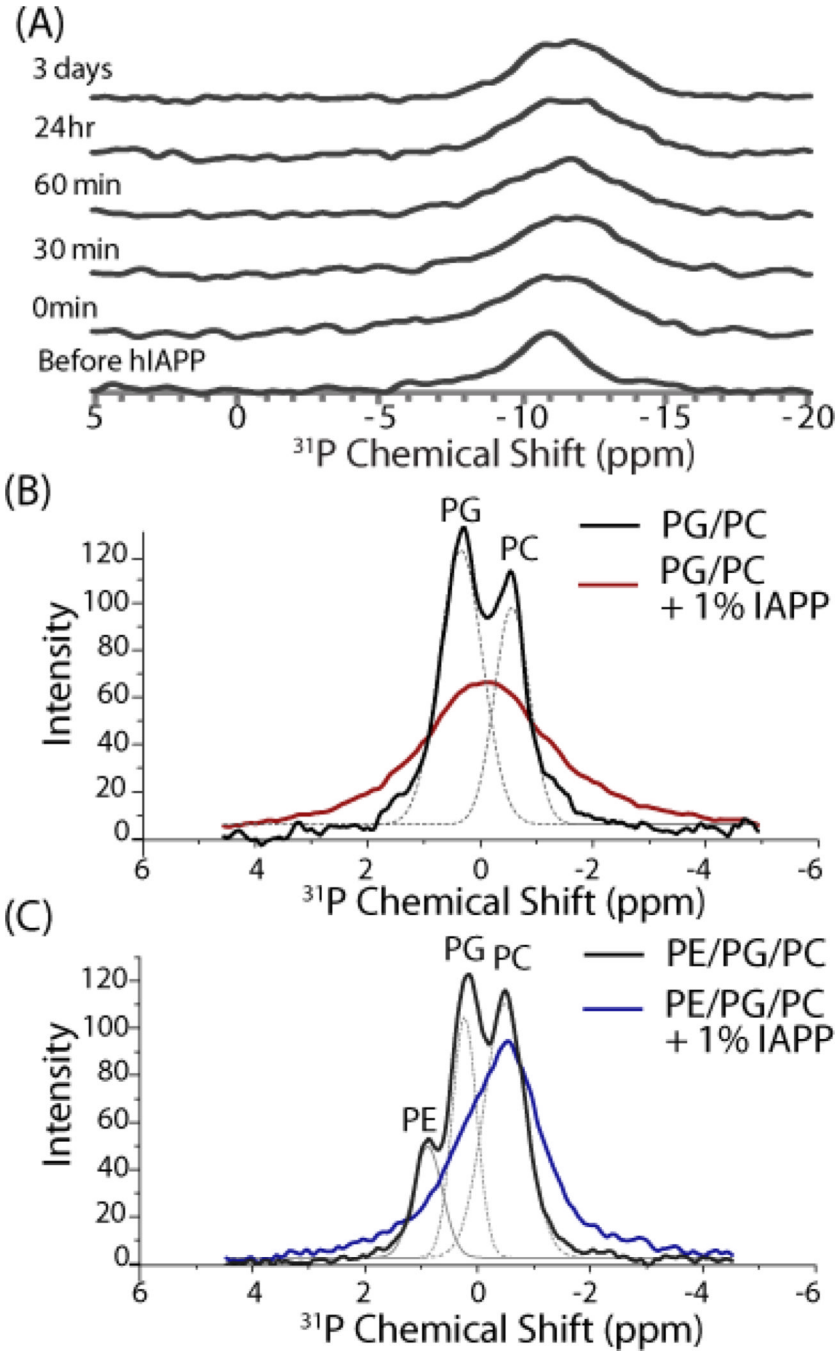

Figure 5.

^{31}P NMR spectra revealing the interaction of IAPP amyloid fibers with lipid vesicles. **(A)** Time dependent static ^{31}P NMR spectra of aligned bilayers after the addition of 1 mole % IAPP. Changes are not apparent in subsequent spectra after the addition of IAPP, suggesting IAPP reached the amyloid state before the first spectra was acquired. **(B and C)** Magic-angle spinning ^{31}P NMR spectra of multilamellar vesicles **(B)** 7/3 POPC/POPG and **(C)** 3/4/3 POPE/POPG/POPC) incubated with 1.178 mM (1 mole %) IAPP. Dotted lines represent a deconvolution of the spectrum. Experiments were performed at 37 °C in 10 mM Tris Buffer, 100 mM NaCl, pH 7.4.

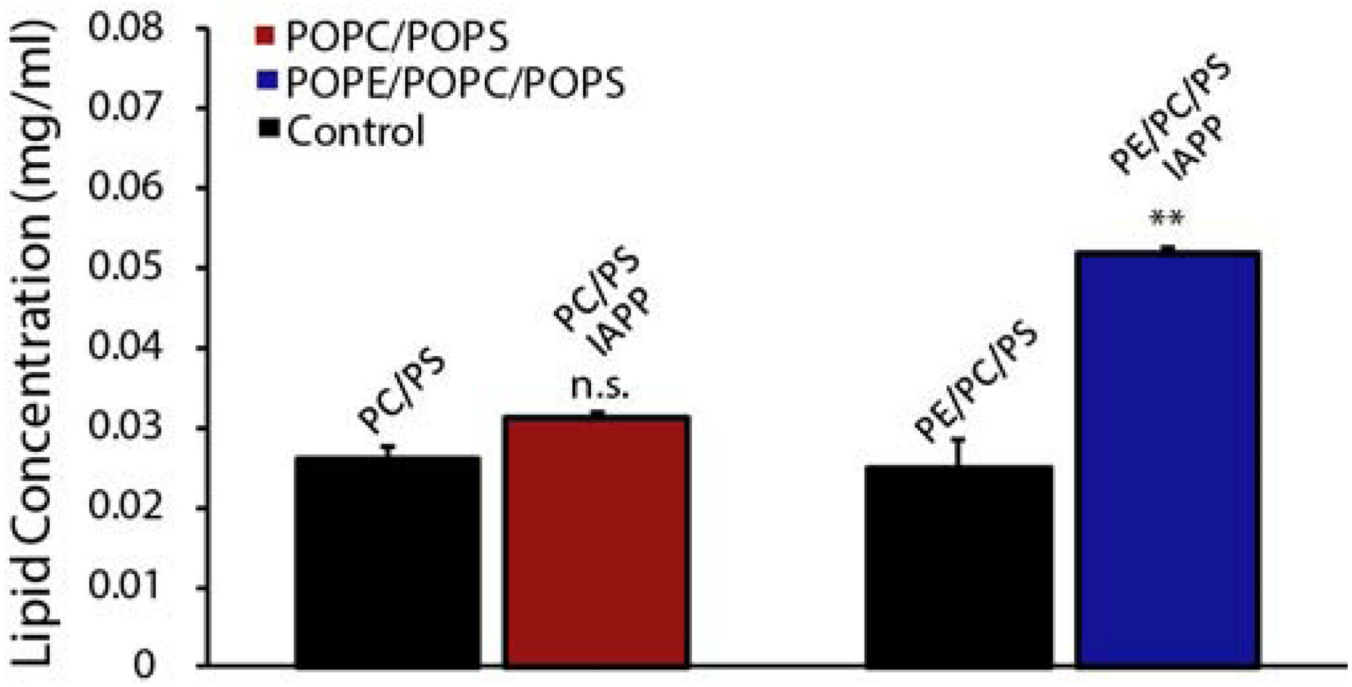

Figure 6.

Membrane fragmentation induced by IAPP. 15 μM IAPP was incubated with 1 mg/ml large unilamellar vesicles before fragmented membranes were separated by centrifugation at 14,000 rpm. Lipid concentrations were measured by the Stewart assay. All experiments were performed in 10 mM phosphate buffer, 100 mM NaCl, pH 7.4. Results are the average of three experiments, error bars indicate the standard error of measurement. The fragmentation of membranes containing PE is significantly higher than those without.

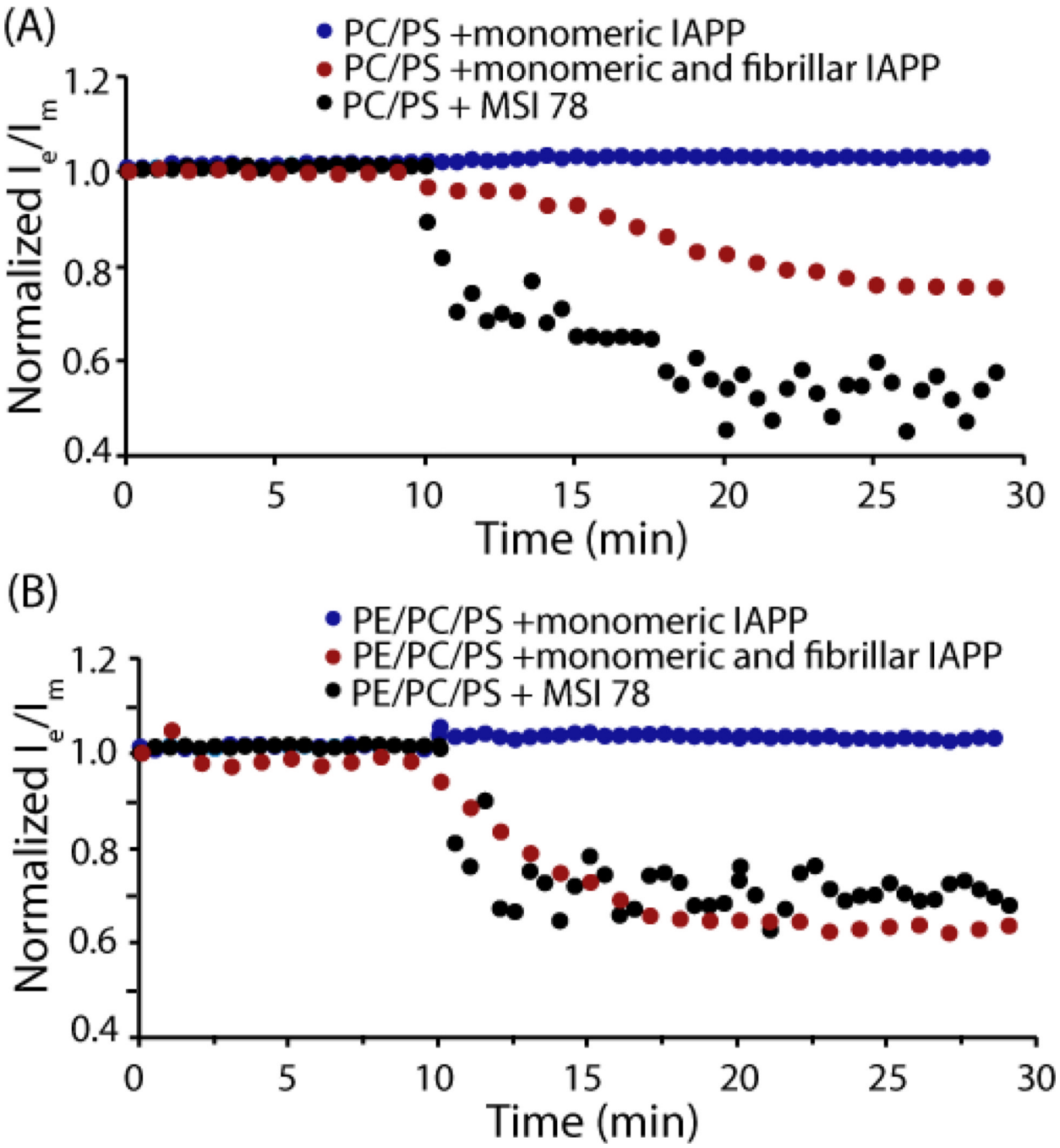

Figure 7.

Loss of membrane asymmetry induced by IAPP measured by the pyrene-PC assay. Lipid translocation induced by 1 μM monomeric IAPP, 1 μM monomeric IAPP in the presence of 1 μM preformed IAPP fibers, and 0.5 μM MSI 78 in 20 μM (A) POPC/POPS 7/3 or (B) POPE/POPC/POPS 3/4/3 large unilamellar vesicles labeled with 3% PyPC in the outer leaflet. Both peptides were added at the 10 minute mark. All experiments were performed at 37°C in 10 mM phosphate buffer, 100 mM NaCl, pH7.4.